ARTICLE OPEN

Check for updates

Transabdominal ultrasound guided AAV9-GFP delivery in fetal pigs: a translational and minimally invasive model for in utero fetal gene therapy

Alessia Di Donfrancesco[1,7], Alessia Adelizzi[1,7], Anastasia Giri[2], Roberto Duchi[3], Simona Boito[2], Maria Barandalla[3], Giulia Massaro[4], Chiara Santanatoglia[5], Enrica Cappellozza[5], Andrea Perota[3], Ivano Di Meo[1], Valeria Tiranti[1], Emanuela Bottani[5], Cesare Galli[3], Nicola Persico[2,6]✉ and Dario Brunetti[1,6]✉

In utero fetal gene therapy (IUFGT) has the potential to correct severe monogenic disorders before irreversible damage occurs. Despite promising results in small and large animal models, its translation to clinical practice remains limited by technical challenges, safety concerns, and the lack of standardized protocols in relevant disease models species. We established and validated a minimally invasive, ultrasound-guided approach for systemic gene delivery in fetal pigs using a self-complementary AAV9 vector encoding GFP under a CAG promoter. Injections were performed at different gestational ages (GA 80 and GA 108) via intracardiac or umbilical venous routes. Postnatal outcomes were monitored, and transgene biodistribution and expression were assessed by qPCR, ddPCR, immunofluorescence, and Western blotting. Inflammatory response, toxicity, and maternal safety were evaluated through cytokine profiling and histological analyses. The procedure was well tolerated, with no significant maternal morbidity or adverse obstetric outcomes beyond one preterm delivery. Biodistribution analysis revealed widespread vector presence in peripheral tissues, with robust GFP expression in liver and heart. Importantly, there was no evidence of significant tissue toxicity, necrosis, or fibrosis in any of the organs analyzed. Mild increases in pro-inflammatory cytokines (GM-CSF, GRO-α, IFN-γ) were observed but were not associated with histopathological changes. No anti-AAV9 capsid antibodies were detected in sera from piglets or sows, suggesting a minimal immune response to the vector. These findings demonstrate the safety, feasibility, and efficacy of ultrasound-guided IUFGT in pigs, supporting its potential as a translational platform for therapeutic gene delivery in fetuses affected by severe congenital diseases. This model offers a valuable framework for further preclinical development of prenatal interventions, particularly for disorders with early onset, such as mitochondrial diseases.

Gene Therapy; https://doi.org/10.1038/s41434-025-00551-8

INTRODUCTION

Gene therapy has rapidly evolved as a transformative treatment for inherited diseases. The first in vivo gene therapy approved in the West was Glybera for lipoprotein lipase deficiency [1]. This paved the way for other therapies like Luxturna (inherited retinal dystrophy) [2], Zolgensma (spinal muscular atrophy) [3], Roctavian and Hemgenix (haemophilia A and B) [4, 5], and Elevidys (Duchenne muscular dystrophy) [6]. These treatments have significantly improved patient quality of life and altered the natural course of diseases, revealing previously unknown aspects masked by early mortality.

For many early-onset genetic disorders, early intervention is key to efficacy. Some trials revealed a significant improvement in the course of the disease, whereas others have shown poor efficacy and unforeseen toxicity. In some conditions, the poor efficacy of postnatal gene therapy depends on the fact that the pathogenesis begins prenatally [7].

Among viral vectors, adeno-associated viruses (AAVs) are widely used due to their safety [8, 9], and efficiency. AAVs can infect dividing and non-dividing cells and persist extrachromosomally despite recent studies have shown that if administered at high doses it can integrate into the host's genome [8]. These characteristics render AAVs appealing candidates for the safe and effective delivery of therapeutic genes [9]. However, the broad clinical application of AAVs might be limited by the high cost of large-scale AAV manufacturing [10] and by the existence of natural immunity, marked by the presence of anti-AAV capsid antibodies or cytotoxic T cells induced by previous infections of natural wild-type (wt) AAV in humans [11].

All the above-mentioned issues can be, in theory, bypassed or attenuated by in utero fetal gene therapy (IUFGT).

IUFGT represents a groundbreaking frontier in the field of medical science, offering the potential to address genetic

[1]Unit of Medical Genetics and Neurogenetics, Fondazione IRCCS Istituto Neurologico "Carlo Besta", Milan, Italy. [2]Prenatal Diagnosis and Fetal Surgery Unit, Fondazione IRCCS Ca' Granda, Ospedale Maggiore Policlinico, Milan, Italy. [3]Avantea Laboratory of Reproductive Technologies, Cremona, Italy. [4]UCL School of Pharmacy, University College London, WC1N1AX, London, UK. [5]Department of Diagnostics and Public Health, University of Verona, Verona, Italy. [6]Dipartimento di Scienze Cliniche e di Comunità, Dipartimento di Eccellenza 2023-2027, University of Milan, Milan, Italy. [7]These authors contributed equally: Alessia Di Donfrancesco, Alessia Adelizzi. ✉email: nicola.persico@policlinico.mi.it; dario.brunetti@istituto-besta.it

Received: 20 February 2025 Revised: 13 May 2025 Accepted: 26 June 2025
Published online: 11 July 2025

abnormalities and congenital disorders at their earliest stages of development. Unlike traditional gene therapies administered postnatally, IUFGT aims to deliver genes to cells and tissues early in prenatal life, offering the potential of prevention, allowing the correction of a genetic defect before early irreversible tissue damage has occurred and, overall, improving or mitigating postnatal clinical outcomes [12].

In contrast to postnatal gene therapy, the prenatal application may offer several advantages such as the small fetal size that allows for a higher vector-to-target-cell ratio to be achieved with a notable reduction in the production costs of the virus; the ability to target neurons before the blood-brain barrier (BBB) fully matures increasing brain transduction and thus improving the ability to ameliorate neurologic manifestations and to treat disorders in which irreversible pathological metabolic and molecular changes begin before birth [13]. Another important point concerns the relative immaturity of the immune system which may develop tolerance to persistent antigens (e.g., therapeutic transgene products). Notably, transient antigens such as AAV capsid proteins are unlikely to induce long-term tolerance, even when delivered in utero [13, 14]. Despite recent advances in fetal surgical techniques, IUFGT is a challenging procedure that requires specific skills and specialized treatment centers. The safety of IUFGT for the mother and fetus must be thoroughly investigated in large preclinical models before proceeding to translation [15]. Over the past years, several authors have mainly used wild type sheeps [16] and non-human primates (NHP) [17–20] as models for the development of AAV mediated IUFGT technique focusing on long-term transgene expression and immunological response. However, both species are less amenable to the development of genetically modified (GM) models that mimic human diseases. This has been an obstacle in demonstrating the real efficacy of IUFGT in preventing or mitigating the onset of a genetic disease. The pig has been increasingly used as a suitable animal model in various biomedical research programs. Pigs share several anatomic, physiological, genetic, and metabolic features with humans, making them a favorable animal model for translational medicine [21] and often used for studying neurodegenerative or metabolic disorders. In addition, new genome editing technologies, combined with somatic cell nuclear transfer, have recently increased the use of GM pigs in biomedical research as a valid alternative to non-human primates which have high costs and ethical limitations [22]. Here, we described a minimally invasive protocol to test IUFGT in a fetal pig model, using ultrasound-guided delivery of an adeno-associated virus carrying the green fluorescent protein transgene (scAAV9-CAG-GFP).

METHODS

Animals

All procedures involving the use of animals in this study were approved by the Local Ethics Committee of Avantea, carried out under the Italian Law (D. Lgs 26/2014) and EU directive 2010/63/EU regulating animal experimentation, and approved by the relevant national authorities (Ministry of Health project n° 367/2022-PR). All the animal studies were done according to the ARRIVE guidelines.

Chemicals

Unless otherwise stated, all chemicals and reagents were purchased from Sigma-Aldrich (Milan, Italy).

Viral construct

The psAAV-CAG-GFP vector was a gift from Mark Kay (Addgene plasmid # 83279; http://n2t.net/addgene:83279; RRID: Addgene_83279).

The integrity of inverted terminal repeat (ITR) sequences was checked by enzymatic restriction digestion with AhdI and XmaI. AAV vector particles were generated in HEK293T cells culture in roller bottles by a cross-packaging approach whereby a helper plasmid encoding adenovirus E4, E2A and VA and a packaging plasmid encoding AAV Rep and the capsid proteins which determine the specific serotype are transfected in conjunction with the vector plasmid.

Viral stocks were obtained by PEG precipitation and two consecutive CsCl2 gradient centrifugation. The physical titer of recombinant AAVs was determined by quantifying vector genomes (vg) packaged into viral particles, by real-time PCR against a standard curve of a plasmid containing the vector genome; values obtained were in the range of 1×10^{12} to 1×10^{13} vg per milliliter.

Animal care and trans-abdominal ultrasound-guided vector injection

Four artificially inseminated (AI) sows were used in this study. Sows' oestrus was synchronized by feeding 12 mg of altrenogest (Regumate, Intervet, Peschiera Borromeo, Italy) *per* sow for 15 days, paralleled by an intramuscular injection of 0.15 mg of PgF2α (Dalmazin, Fatro, Ozzano Emilia, Italy) at the 13th day of altrenogest treatment and one of 1000 IU of hCG (Chorulon, Intervet, Peschiera Borromeo, Italy) 96 h after the last altrenogest treatment. Inseminations were done on the 15th day of altrenogest treatment when estrus behavior was evident.

Sows were checked for pregnancy by trans-abdominal ultrasound examination 30 days after AI and pregnancies were confirmed around day 60 post-AI. Each sow received a single scAAV injection at different gestational ages (GA) ranging from 80 days post AI to 108 days post AI.

On the day of AAV delivery, the sows were first sedated with an intramuscular (IM) injection of 2 mg/Kg Azaperone (Stresnil, Elanco Italia S.p.A., Milano Italy) and anesthetized with IM injection of 0.5 mg/Kg Zoletil (tiletamine hydrochloride and zolazepam hydrochloride, Virbac srl Milano Italy).

Sows were then maintained under general anesthesia via a face mask connected to a mechanical ventilator, delivering 1.5% isoflurane mixed with oxygen and nitrous oxide at 4 L/min for the procedure. The sow was placed on a stretcher with her abdomen facing upwards. The skin was soaped, hair removed and then disinfected with iodine povidone (10%) solution followed by another round of skin disinfection with an alcholic solution (70%). A sterile ultrasound gel was then spread on the abdominal skin.

A Voluson S8t BT22 ultrasound system was used to identify the location and orientation of fetal piglets. We tested two different routes of administration: (1) intracardiac injection in the left ventricle or (2) intra umbilical vein injection, performed near the placental cord insertion using a 20-gauge spinal needle. The entire injection procedure was conducted under ultrasound guidance, which included identifying the collection site, visualizing needle insertion, confirming turbulent flow during the injection into the fetuses, and ensuring adequate recovery. Following the procedure, the cardiac activity of each fetus was monitored for two minutes and the sow was carefully supported during anesthesia recovery. Post-surgery, all animals were closely monitored on a daily basis.

A subcutaneous injection of flunixin meglumine 2,2 mg/kg (Alivios Fatro, Ozzano Emilia, Italy) was administered for analgesia; amoxicillin 0,1 mL/kg (Clamoxyl Long Acting, Zoetis Italia srl, Roma, Italy) was administered to prevent eventual sepsis. At the end of the surgical procedure sows also received an intramuscular injection of prednisolone acetate 1 mg/kg (Novosterol, Ceva Salute Animale spa, Milano, Italy) daily until the delivery to reduce the eventual viral *prep* immunogenicity (research grade prep often present a lower degree of purity compared to clinical grade and may contain immunogenic elements). Farrowing was induced by a PgF2α injection on day 115 of gestation.

Molecular analyses

Total DNA was extracted from frozen tissues using an automated DNA extraction kit (Promega, United States, AS1120). The presence of vector DNA was verified in tissues by PCR using 100 nM of each primer designed to detect GFP. The following primers were used: eGFP-Forward: 5′-CACATGAAGCAGCACGACTT-3′; eGFP-Reverse: 5′- TCCTTGAAGTC-GATGCCCTT-3′. Digital droplet PCR (ddPCR) was used to quantify the AAV copies/cells in postnatal tissues based on the amplification of the eGFP gene and the GCG gene (NC_010457.5). The following primers were used: eGFP-Forward: 5′-GAGCAAAGACCCCAACGAGA-3′; 5′-CTCCACCCATA-GAATGCCCAGT-3′. Extracted DNA was quantified using Qubit™ 1X dsDNA High Sensitivity (HS) and Broad Range (BR) Assay KitsGreen (Invitrogen, Catalog number: Q33231) with specific Qubit™ Assay Tubes (Invitrogen, Catalog number: Q32856). The amplification reaction was prepared with

20 ng of purified DNA, 100 nM of each primer, ddPCR Evagreen Supermix, and 1U/reaction of AatII enzyme (Roche Diagnostics GmbH - Mannheim, Germany). The reaction was then fractionated into ~20,000 droplets on a QX200 Droplet Generator and end-point PCR was performed. Cycling steps for the ddPCR were as follows: initially, an enzyme activation at 95 °C for 5 min (1 cycle) followed by 40 cycles of denaturation and annealing/extension (each cycle at 95 °C for 30 s and 60 °C for 1 min) and finally signal stabilization (4 °C for 5 min and 90 °C for 5 min, 1 cycle). Droplets were read on a droplet reader and data were analyzed using QuantaSoft™ Software. The fraction of positive droplets was fitted to a Poisson distribution in QuantaSoft™ Software to determine the absolute copy number in units of copies/µL. To determine the GFP copy number per cell, the following calculation was performed:

GFP copy number per cell = (GFP copies/CGC copies)*2

Immunoblotting

Pig tissues were homogenized in 10 volumes of cold 1X RIPA buffer supplemented with protease and phosphatase inhibitors from Roche (Switzerland), incubated 30 min on ice and then centrifuged at 14,000 rpm at 4 °C for 30 min. Following three freeze-thaw cycles, the protein concentration in the resulting supernatant was determined using the Bradford protein assay kit from Biorad (CA, United States, 5000006). For gel electrophoresis, 60 µg of each protein lysate was loaded onto a polyacrylamide gel with a density gradient of 4% - 12%. The proteins were then transferred onto a nitrocellulose membrane. Blocking was performed for 1 h with 5% milk powder (Blotting-Grade Blocker #1706404 Biorad) or 5% BSA (#A5611, Sigma) in TBS with 0.1% Tween-20 (TBST). The membranes were incubated overnight with primary antibodies diluted in the appropriate blocking solution at 4 °C. Subsequently, the membranes were incubated with corresponding HRP-conjugated secondary antibodies from Sigma-Aldrich (MO, United States) for 1 h at room temperature. Visualisation of the proteins was achieved using either Clarity Western ECL Substrate (1705061) or Clarity Max Western ECL Substrate (1705062) from Biorad (CA, United States), and the images were captured with the Azure Biosystem Aerogene 300Q imaging system. Densitometric analysis was performed using ImageJ software: after background subtraction, the signal intensity of each band of the protein of interest was normalised to those of the corresponding loading controls (Beta Actin ACTB). Primary antibodies used included rabbit anti-GFP (1:1000 Invitrogen #ab-11122, United States), anti-ACTB (1:1000, Abcam #ab18226, UK). Secondary antibodies include ECL anti-mouse IgG peroxidase (Sigma- Aldrich, GENA931) and ECL anti-rabbit IgG peroxidase (Sigma- Aldrich, GENA9340).

Immunological analyses

The presence of binding Abs reactive against the AAV vector capsid was determined by semiquantitative indirect enzyme-linked immune-sorbent assay (ELISA) technology, following manufacturer's instructions (Creative Diagnostics, United States # DEIASL348). AAV9 capsid protein was precoated onto 96- well plates. Absorbance at 450/620 nm was read in duplicate experiments using an ELISA Microplate reader. The cytokine antibody array (Abcam, ab133997) was used to determine the change in expression of 42 cytokines tissue samples of GFP positive piglets compared to controls.

Liver lysates have been prepared using the cell lysis buffer included in the kit to which protease inhibitor has been added. After extraction, lysates have been clarified by centrifugation and the supernatant used for the experiment. 300 ug of total protein have been used in 1 mL of 1X Blocking Buffer (final volume) for each array membrane. Samples were incubated overnight at 4 °C, 1X Biotin-Conjugate Anti-Cytokines and 1x HRP-Conjugated Streptavidin for 2 h at RT. A CCD camera was used for detection. Cytokine quantification was performed using Image Lab software version 6.1 (Bio-Rad Laboratories) to analyze the detected images. Regions of interest (ROIs) were defined to match the dimensions of each well on the array membrane. A volume table was generated, and the signal intensity for each cytokine was averaged across samples within the same experimental group. The cytokine concentrations are reported as fold changes relative to the control group.

Histological analyses

After sacrifice, tissues from scAAV9-CAG-GFP-injected animals were immediately removed, post-fixed in paraformaldehyde 4% at 4 °C for 48 h, crioprotected in phosphate-buffered saline containing 30% sucrose for 24 h at 4 °C and then frozen in optimal cutting temperature compound (OCT) in dry ice. Ten-micrometer-thick cryostat sections were mounted and collected on gelatinated glass slices. For histological analysis, sections were stained with hematoxylin-eosin, Periodic acid-Shiff reaction (PAS) and the negative control PAS with diastase. A complete kit (Bio-Optica #04-010802) was used for the Masson trichrome straining. The sections were visualised and acquired under a light microscope (Nikon Eclipse E400) using 20X or 40X magnification.

For immunofluorescence analyses, sections were incubated with rabbit anti-GFP (1:500), anti-Iba1 (1:200), or anti-GFAP (1:1000) overnight at 4 °C. The sections were then washed three times with phosphate-buffered saline and stained with Alexa Fluor 488-conjugated goat anti-rabbit IgG (1:1000, Invitrogen, Monza (MB), Italy), Alexa Fluor 568-conjugated goat anti-mouse (1:1000, Invitrogen) and hoechst 33342 nucleic acid stain (1:1000, ThermoFisher, Monza (MB), Italy). Finally, the sections were acquired using a TCS-SP8 laser confocal microscope (Leica, Buccinasco (MI), Italy).

Statistical analysis

All numerical data are expressed as mean ± s.d. Student's unpaired two-tail *t*-test and two-way ANOVA were used for statistical analysis. Differences were considered statistically significant for $p < 0.05$.

RESULTS

Transabdominal ultrasound-guided in-utero injection of scAAV9-CAG-GFP

We developed a minimally invasive, ultrasound (US)-guided technique for delivering AAVs to fetal piglets in utero. This approach, akin to standard procedures in fetal medicine such as blood transfusion, can be readily adapted for clinical application (see Experimental section for details).

We performed four rounds of in-utero injections in four pregnant sows ranging from gestational age (GA) 80–108 (pig gestation is ~115 days), corresponding to the beginning of the third trimester to the end of the third trimester in humans [23].

Under direct ultrasound visualization, the operator inserted a 20-gauge spinal needle at a 45° angle relative to the ultrasound beam. The needle was guided through the maternal skin, the uterus, and into the amniotic cavity (Fig. 1a). The needle was then inserted in the umbilical vein near the placental cord insertion (Fig. 1b and Supplementary Video 1) or in the fetal heart chamber of the left ventricle (Fig. 1c and Supplementary Video 2) to deliver the virus. The entire procedure, including intubation and surgical preparation of the sow, fetal identification, and virus injection, had an average duration of 28 min. Fetuses received injections of scAAV9-CAG-GFP ($n = 7$) or saline ($n = 2$).

The viral doses injected into the fetuses ranged from 1.2×10^{12} viral genomes (vg)/kg to 5×10^{13} vg/kg, resuspended in 1–2 mL of sterile saline solution. Experimental details are summarized in Table 1. After the procedure, the cardiac activity of each fetus was monitored for 2 min, then re-checked 10 min later, and found to be normal in all injected fetuses.

Farrowing, clinical, and necroscopic assessment

Injections performed at GA 80 resulted in premature labor 16 days later (GA 96), leading to the delivery of 15 fetuses. All of them displayed similar developmental stages, with comparable weight and length (Supplementary Table S1); no macerated or mummified fetuses were found. These findings suggest that there was no fetal death in the hours following the procedure, but the pregnancy continued normally for 16 days until the preterm labor.

The other three sows injected at GA 108 presented a normal farrowing on GA 115, delivering a total of 37 alive piglets and 6 stillborn piglets (Supplementary Fig. S1a).

PCR analysis on DNA extracted from tail biopsies revealed that three alive piglets (#720; #725 and #779) and two stillborn piglets were GFP-positive (GFP^+ Supplementary Fig. S1b), and the GFP expression in tail's biopsies was also confirmed by visualization

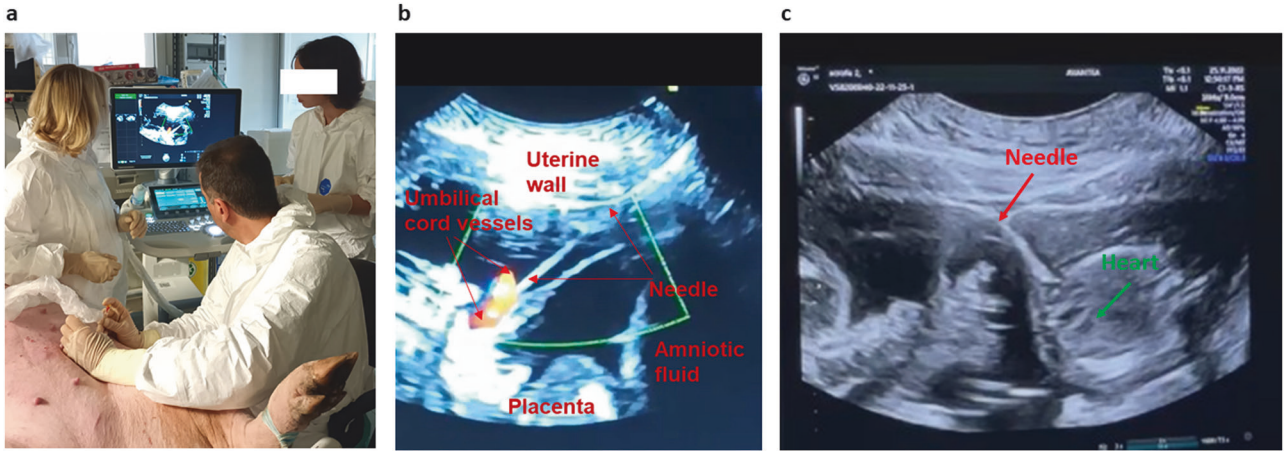

Fig. 1 Ultrasound-guided, in-utero fetal injection procedure in pigs. a Representative image of the transabdominal injection. **b** Ultrasound image of the scAAV9-CAG-GFP injection in the fetal umbilical vein. **c** Ultrasound image of intracardiac scAAV9-CAG-GFP injection.

under a fluorescent stereomicroscopy using the GFP filter ($\lambda_{ex} =$ 488 nm, $\lambda_{em} = 530$ nm) (Supplementary Fig. S1c). All the GFP$^+$ piglets, either alive or stillborn had a normal birth weight, indistinguishable from those of GFP-negative littermates (Supplementary Fig. S1d) and in line with the average weight of untreated wilde type neonatal piglets of the same strain in our facility. The two GFP$^+$ stillborn piglets showed no signs of post-mortem or degenerative changes, such as discoloration of the skin and loss of fluids, but appeared normal, suggesting that the pigs died during the farrowing. Alive piglets (ID #720; #725 and #779) presented a regular suckling and rooting reflex; no sign of distress, lethargic phenotype, or pyrexia (Supplementary Fig. S1e) were observed compared to controls. Urine analysis revealed no alterations compared to age-matched controls (Supplementary Table S2). The #779 piglet was sacrificed 3 days after birth. During necropsy procedures, green fluorescence of the internal organs was observed (as in the stillborn piglets) when exposed to a UV lamp (Supplementary Fig. S2b). Organ weights of either alive or stillborn piglets normalised to body weight were comparable to those of uninfected, control littermates of the same age (0–3 days) (Supplementary Fig. S2c), and no macroscopic evidence of inflammatory or toxic signs was observed.

GFP$^+$ piglets #720 and #725 were left to grow until one month of age. Their growth and behavior were comparable to un-injected siblings. No signs of distress, immune reactions (pyrexia, pain, redness, or swelling) or lethargic phenotypes were observed.

None of the sows used in the four experiments developed fever, sepsis or external inflammatory signs after the procedure. At necropsy, the uterus, liver, and lymph nodes appeared normal.

scAAV9 biodistribution and GFP expression

The transduction efficiency was evaluated by analyzing the tissue distribution of the scAAV9 genome in fetal, neonatal, and one-month-old piglets, through PCR and digital droplet PCR (ddPCR) on DNA extracted from tissue biopsies, revealing a widespread expression of the transgene in different organs.

At the fetal stage, PCR analysis detected a GFP transgene amplicon in all tissues of fetus 1 and fetus 4 (Fig. 2a). ddPCR analysis quantified scAAV9 copies *per* cell in the liver (mean ± SD: 21.69 ± 25.7 vg/diploid genome), heart (0.185 ± 0.0775 vg/diploid genome), brain (0.02 ± 0.014 vg/diploid genome), muscle (0.065 ± 0.049 vg/diploid genome) and kidney (0.31 ± 0.268 vg/diploid genome) (Fig. 2b).

Accordingly, Western Blot analysis revealed a higher GFP expression in the liver, heart, and kidney, and a mild expression in skeletal muscle and brain (frontal cortex) (Fig. 2c). These results were also confirmed by immunofluorescence (Fig. 2d), suggesting that the dose of 4.5×10^{12} vg/kg conferred a good biodistribution and transgene expression at least sixteen days after injection.

In newborn and stillborn piglets, GFP was detected by standard PCR in several tissues (Fig. 3a). ddPCR was used to quantify the AAV9 copies per cell in the liver (mean ± SD: 31 ± 20 copies/cells), heart (2.66 ± 0.35 copies/cells), spleen (4.11 copies/cell), and lungs (4.44 copies/cells). AAV9 also reached the skeletal muscle, kidney, and the brain where, however, the efficiency of infection was lower (0.22 ± 0.337 copies/cell; 0.17 ± 0.136 copies/cell, and 0.113 ± 0.091copies/cell, respectively) (Fig. 3b), possibly reflecting a mixed population of AAV9-positive and -negative cells. Accordingly, Western Blot analysis showed a robust GFP expression in the liver, heart, lungs, and spleen and a moderate expression in muscle, kidney, and different areas of the brain (Fig. 3c). These results were also confirmed by immunofluorescence using an anti-GFP antibody (Fig. 3d).

In one-month-old piglets, ddPCR analysis showed a weak biodistribution of the transgene that was only detected in the liver of pigs #720 and #725 and in the heart of pig #725 (Supplementary Fig. S3). WB or ICC could not detect the low GFP signal in these tissues.

Assessment of anti-AAV antibody responses

One of the major challenges in AAV-based gene therapy is the presence of circulating anti-capsid neutralizing antibodies (NAbs), which can pre-exist in patients as well as in pigs, and may prevent successful gene transfer. Moreover, high levels of circulating anti-neutralizing antibodies can develop after a single administration of gene therapy, preventing the possibility of a subsequent second treatment.

To determine the presence of pre-existing NAb to scAAV9 viral particles in our pig facility, we first measured the presence of NAb by ELISA in the serum of a sentinel sow (SOW S) and of three untreated newborn piglets. All tested animals resulted negative (Fig. 4a). Since this is a barriered facility, this result shows that there were no circulating AAVs among our animals prior to injection.

To understand whether in utero administration of scAAV9-CAG-GFP triggered an immune response, we measured NAb in the serum of piglets (GFP$^+$ and controls) and relative sows at birth and in one-month-old piglets (Fig. 4a). Also in this case, the assay found no detectable levels of NAb in any of the animals tested.

Evaluating the potential for inflammatory effects after in utero gene therapy

Inflammatory mediators like interferons and pro-inflammatory cytokines are frequently generated in reaction to viral infections, including those associated with AAV vectors. Understanding these

Table 1. Experimental details of ultrasound-guided in utero injection procedures in piglets.

	Experiment			
	SOW1	**SOW2**	**SOW3**	**SOW4**
GA (days)	80	108	108	108
Injected Fetuses	2	2	2	3
Dose (vg/Kg)	4.5×10^{12}	5×10^{13}	(1x) Saline (1x) 2.5×10^{13}	(1x) Saline (2x) 1.5×10^{12}
Route	(1x) u.v. (1x) i.c.	i.c.	i.c.	(1x) u.v. (2x) i.c.
Volume (ml)	1	2	2	1
Surgical duration (min)	30	20	20	45
Delivery day	96	115	115	115
Litters	15	16	11	16

GA gestational age, *vg* vector genomes, *i.c.* Intracardiac, *u.v.* umbilical vein.

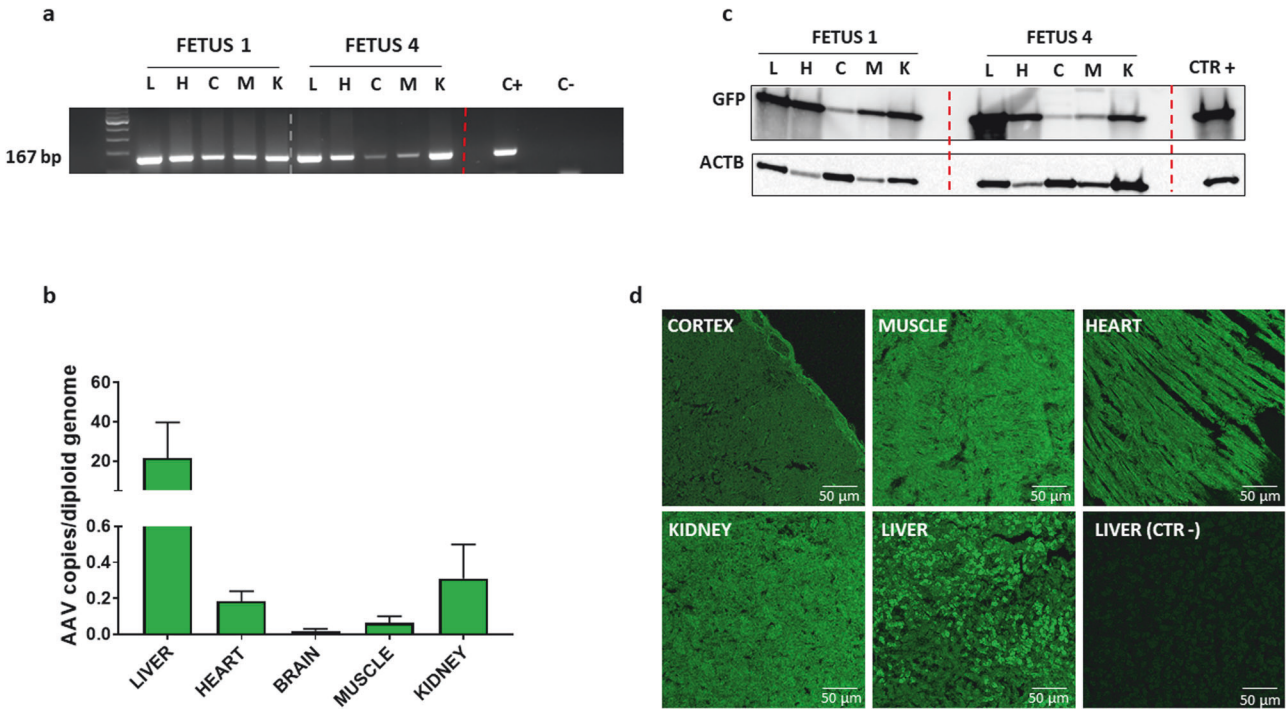

Fig. 2 Representative images of GFP biodistribution and expression in tissues of injected fetuses. a PCR amplified GFP sequence was detected in different anatomical regions of fetus 1 and fetus 4. **b** Viral genome copies (gc) content in tissues from AAV9-treated fetuses ($n = 2$). **c** Western blotting of GFP expression in various peripheral tissues of pigs. Actin B (ACTB) served as a loading control. **d** Immunofluorescent staining showed that GFP was expressed in brain (cortex) and peripheral tissues of pigs after scAAV9-CAG-GFP injection. Regions are: liver (L), heart (H), cortex (C), muscle (M), kidney (K). Scalebar, 50 µm.

immune responses is essential to evaluate the safety and efficacy of AAV-based gene therapies.

Recent preclinical studies have reported rAAV-related inflammatory toxicities in large animal models, including hepatic, cardiac, and renal toxicity, as well as neuroinflammation [24–28].

Because the production of inflammatory cytokines is a pathological feature of inflammation in the liver [29, 30] we have analyzed the expression of 42 cytokines in the liver of GFP+ piglets. We found a slight but significant increase only in three cytokines named: granulocyte-macrophage colony-stimulating factor (GM-CSF), growth-regulated alpha protein (GRO-α), and interferon-gamma (IFN-γ) (Fig. 4b). The upregulated levels of these cytokines may suggest the presence of an immune or inflammatory response triggered by the vector (e.g., viral capsid proteins) or by the transgene product recognized as foreign.

Histological analyses performed using hematoxylin & eosin (HE) staining did not reveal any evidence of inflammatory infiltrates or alteration to the liver's cytoarchitecture. Furthermore, hepatocyte function remained unaltered, as demonstrated by normal periodic acid–Schiff (PAS) staining activity (Fig. 5a) observed in GFP-expressing piglets. To evaluate the possible myocardial damage associated with the AAV9-GFP injection [31] and expression, we investigated the presence of inflammatory signs or fibrosis. HE staining revealed a typical morphology of the myocardium structure without hypertrophic or degenerated cardiomyocytes. No signs of lymphocyte inflammatory infiltration were observed by acidic phosphatase (AP) staining. Further, no fibrotic areas were noted in Masson Trichrome (MT) stained sections (Fig. 5b).

Since recent clinical trials using rAAV have reported renal toxicity issues in addition to hepatotoxicity [32], we evaluated the

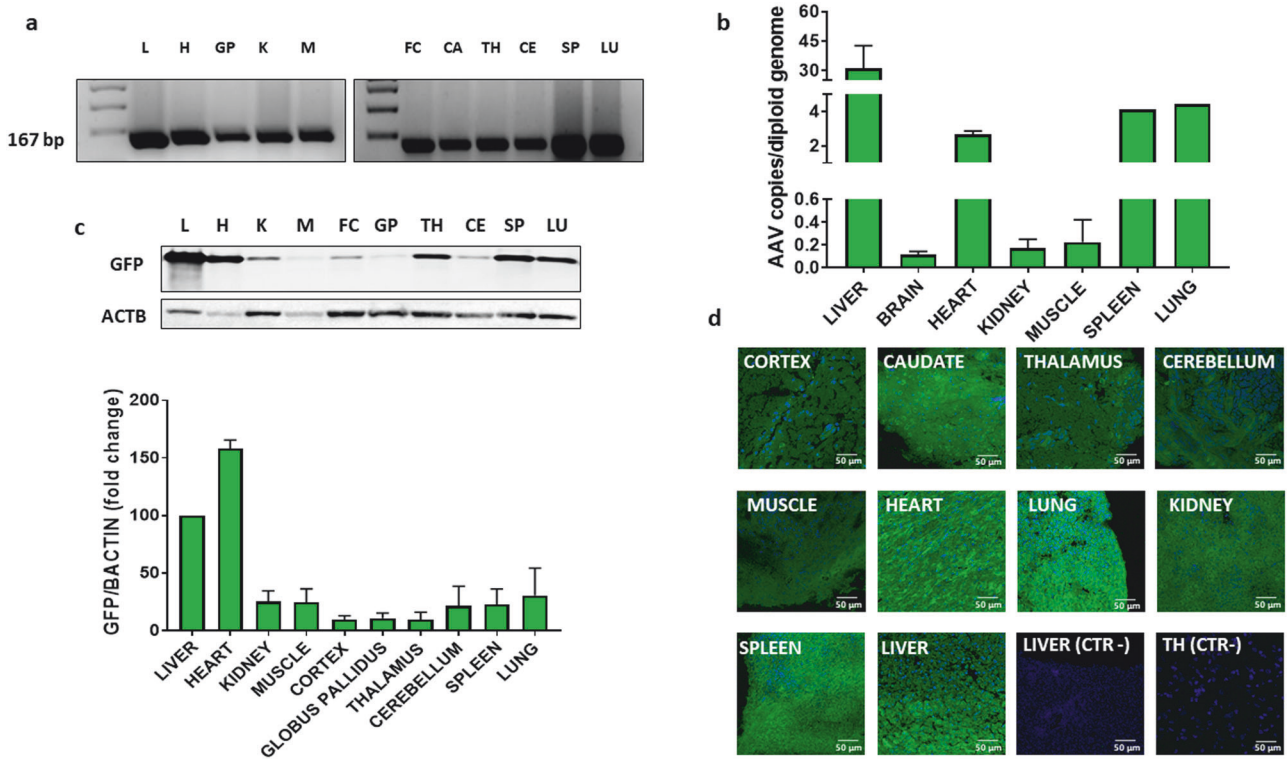

Fig. 3 Representative image of GFP biodistribution and expression in different tissues of pig following transabdominal ultrasound guided injection in the fetal hearth. a PCR amplified GFP sequence was detected in different anatomical regions. **b** Viral genome copies (gc) content in tissues from AAV-treated pigs ($n = 3$). **c** Western blotting of GFP expression in various peripheral tissues of pigs. Actin B served as a loading control. **d** Immunofluorescent staining showed that GFP was expressed in various brain regions and peripheral tissues of pigs after AAV9-GFP injection. Regions are: liver (L), heart (H), globus pallidus (GP), kidney (K), muscle (M), frontal cortex (FC), caudate (CA), thalamus (TH), cerebellum (CE), spleen (SP), lung (LU). Bars indicate the s.d. Scalebar, 50 μm.

kidney morphology of GFP+ and control pigs by HE staining. No obvious signs of inflammation (i.e. accumulation of white blood cells infiltrate or fibrosis) or cell death emerged (Supplementary Fig. S4), in line with normal values observed in urine analysis (Supplementary Table S2).

We then evaluated whether AAV9-GFP expression in the brain may induce neuroinflammation.

To this aim, we evaluated the distribution and the levels of ionized calcium-binding adapter molecule-1 (Iba-1) as marker of activated microglia, and glial fibrillary acidic protein (GFAP) as marker of astrogliosis, by confocal microscopy. No evident differences have emerged between GFP+ and control piglets in the frontal cortex, basal ganglia, thalamus, and cerebellum, suggesting the absence of an inflammatory response in these areas (Fig. 6).

DISCUSSION

Monogenic diseases impact around 1 in 200 pregnancies, constitute at least 80% of rare diseases, and contribute to an estimated ~39 million disability-adjusted life-years (DALYs) based on a 2010 assessment. These conditions are mainly attributed to pathophysiological alterations initiated during the crucial phases of fetal development [33–36].

Congenital disabilities contribute to over 400,000 deaths annually. The prevalence of autosomal recessive diseases is expected to rise with the expanding recognition of rare diseases as genetic syndromes. Additionally, the incidence of fetal diagnosis of monogenic diseases is anticipated to increase with advancements in prenatal screening [36].

Recent preclinical and clinical evidence for genetic diseases, such as hematological disorders (i.e. *Haemophilias, Haemoglobinopathies, Severe Combined Immunodeficiency Syndrome*), neurodegenerative disorders (i.e. *Mucopolysaccharidoses* and *Gaucher type-II*; *Spinal Muscular atrophy*, *Leber congenital amaurosis*, *Muscular Dystrophy*); mitochondrial diseases (i.e. *Leigh Syndrome*, *GRACILE syndrome*); congenital pulmonary disorders (i.e. *Cystic Fibrosis* and *Inherited Surfactant Protein Syndromes*); metabolic diseases (*Glycogen Storage Disease*, *Hereditary Tyrosinaemia*, *Crigler-Najjar syndrome*, *Wilson disease*, *Infantile hypophosphatasia*), suggest that prenatal interventions could prevent or mitigate postnatal disease manifestations with substantial health and cost advantages [12, 37–39].

In this context, in utero fetal gene therapy has emerged as a groundbreaking approach that can potentially address genetic anomalies and congenital disorders at their earliest stages of development. Many proof-of-concept IUFGT studies have been performed in mice due to the large availability of disease models, multiparity, and lower costs. However, from a translational point of view, large animals represent a better model for setting up a precision medicine procedure like IUFGT. For this reason, sheep and non-human primates were used in pioneering IUFGT studies. Nevertheless, both models have only 1–2 fetuses per pregnancy and a reduced availability of genetic models of diseases. In our study, we used the pig as a model to set up an IUFGT technique by transabdominal ultrasound-guided injection of scAAV9-GFP in the umbilical vein or in the heart of fetuses. To the best of our knowledge, only two studies have evaluated the transduction efficiency, distribution pattern, and safety of AAV9 after in-utero fetal systemic injection in pigs.

In the first study, Rich et al. [40] tested a US-guided delivery of AAV9-shSMN, AAV9-GFP, or PBS (dose range: 6.5×10^{12} vg/Kg to 2.0×10^{13} vg/Kg) in domestic pig fetuses at 77–110 days of GA, via hepatic, intravenous, intraperitoneal, and intracerebroventricular routes. In this study, only the AAV groups underwent preterm

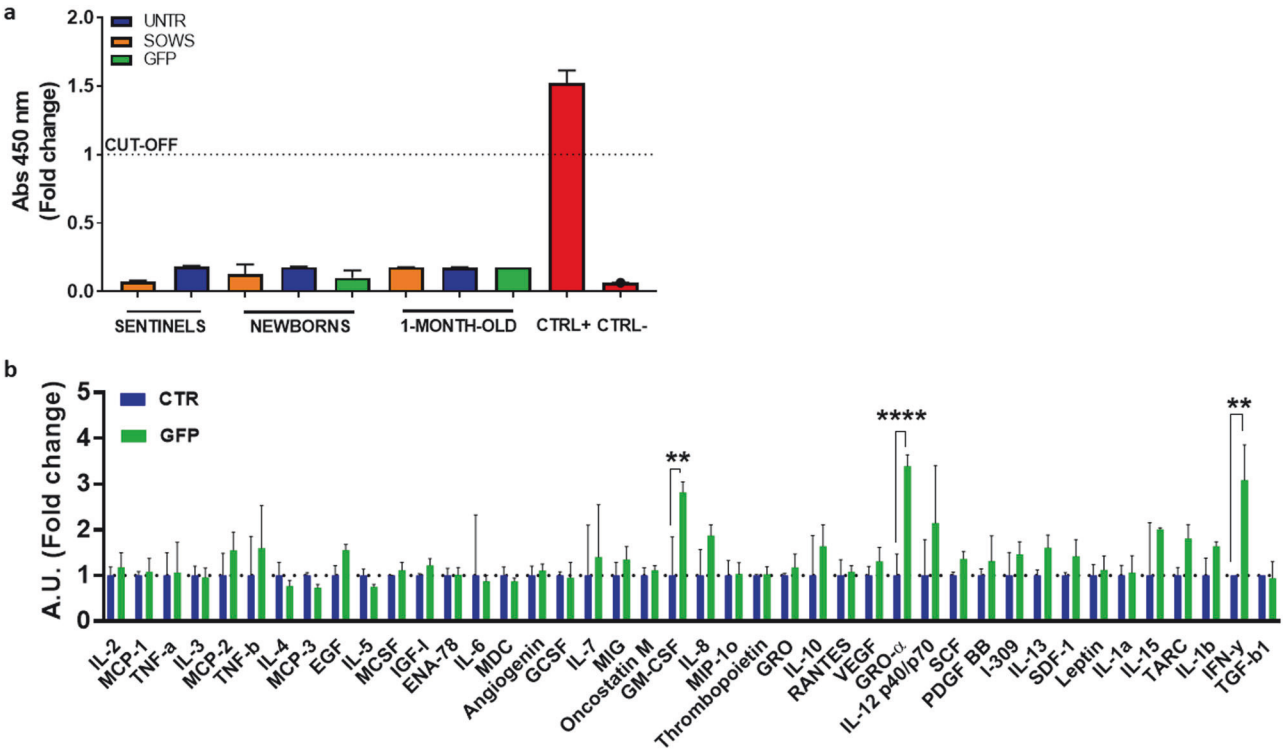

Fig. 4 Evaluation of immune response to fetal scAAV9 delivery. a Assessment of anti-AAV antibodies responses in serum of: sentinel sow and control untreated group; scAAV9-CAG-GFP injected (GA 108) neonatal and one month old piglets and relative sows. **b** Quantification of cytokines fold change in scAAV9-CAG-GFP injected neonatal piglets compared to untreated neonatal controls. Results are shown as mean ± SD. *P*-values are indicated by *<0.05; **<0.01; ***<0.001. Blue columns indicate GFP negative piglets; green columns indicate GFP positive piglets.

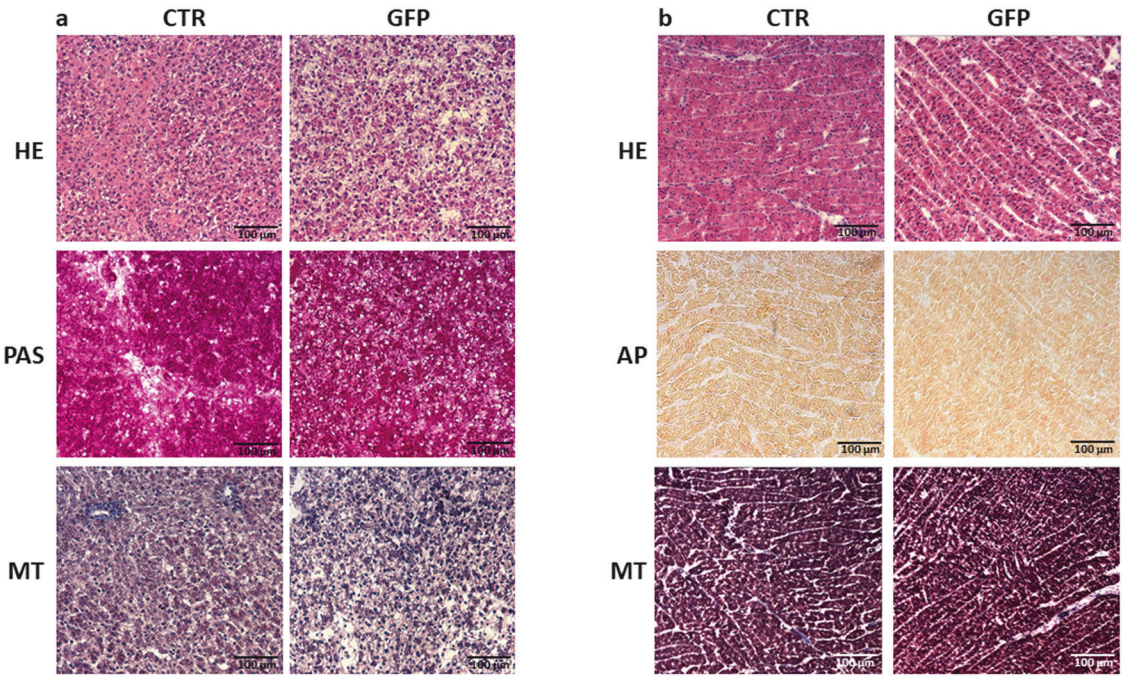

Fig. 5 Histological analysis of liver and heart following fetal scAAV9 delivery. a Histological analysis of liver morphology by HE staining and hepatocytes functionality evaluated by PAS activity; Masson Trichrome (MT) analysis did not highlight fibrotic areas in scAAV9-GFP injected fetuses. **b** Histological analysis of myocardium morphology by HE staining did not reveal significant alterations or inflammatory infiltrations. MT analysis did not highlight fibrotic areas in scAAV9-GFP injected fetuses. Scalebar, 100 µm.

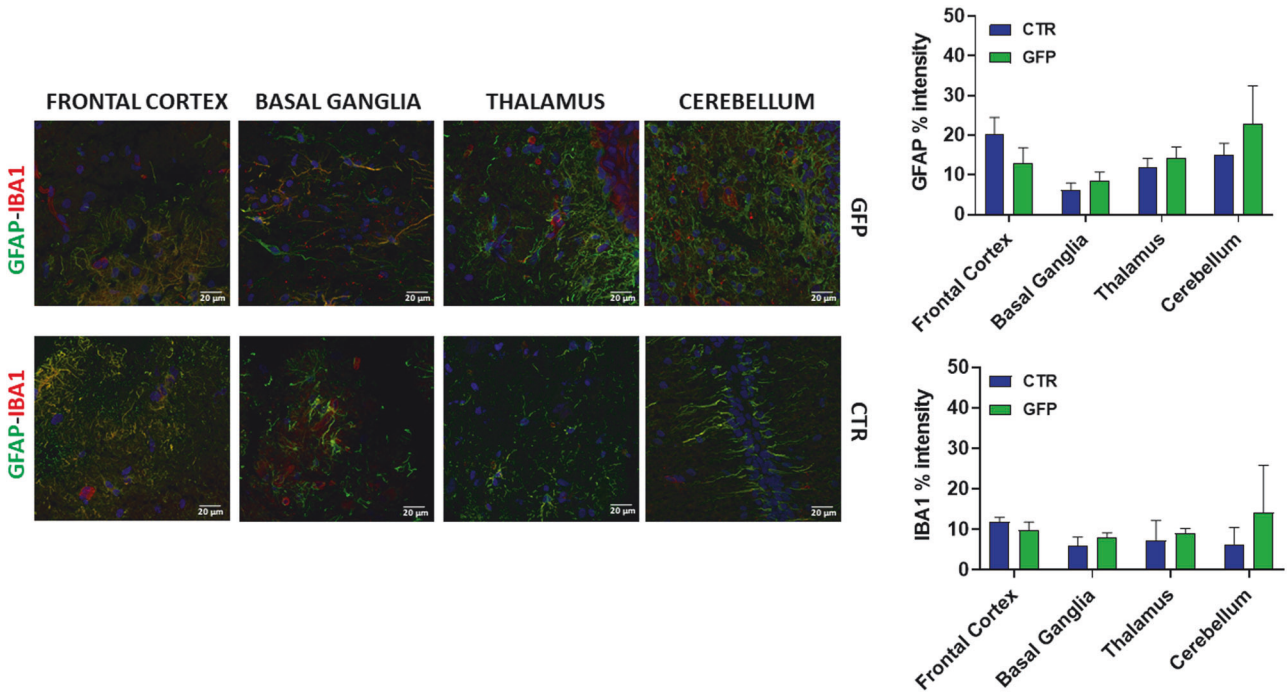

Fig. 6 Double Immunofluorescent staining of astrocytes (GFAP in green) and microglial cells (IBA1 in red) in frontal cortex, basal ganglia, thalamus and cerebellum of scAAV9-GFP injected (#779) vs control piglet (#784). Quantification of these parameters are shown in the graph. Data are means ± SD, unpaired *t*-test, NC not significative. Scalebar, 20 µm.

labor within 1–7 days post-injection in all sows. The authors could not analyze the fetal tissue to quantify the transduction efficiency and evaluate eventual immunological reactions. Consequently, they proposed that either an immune response to AAV9 or the fragility of the multiparous pig pregnancy might be responsible for the preterm delivery. They concluded that the domestic sow might not be a suitable model for preclinical in-utero AAV9 gene therapy studies. In our experience, the prolonged duration of the anesthesia in pigs (in ref. [40] was 103 ± 21 min) correlates with increased risk of hypothermia and stress for the sow with consequent adverse pregnancy outcomes (embryonic reabsorption, fetal death, and increase in stillborn preterm delivery). In our study, the average duration of the anesthesia was 28 min, a drastic reduction compared to the procedure previously described by Rich et al. [40]. This operational speed could have a significant impact on the health of the animals and contribute the favorable outcomes.

In a second study, Parenteau's group performed an open surgical procedure to deliver AAV9-GFP via the umbilical vein in the Yucatan mini-pig. A pregnant sow at 104 days underwent a laparotomy to expose the uterine horn, followed by hysterotomy in the uterine sacs of the fetuses to exteriorize the umbilical cord. Then, a dose of 4.5×10^{13} vg/Kg and 9×10^{13} vg/Kg was injected via cannulation of the umbilical vein. Fetuses were delivered via cesarean section seven days post-procedure (day 111 of GA, four days before the natural gestational term). Authors observed a widespread AAV9-GFP biodistribution in fetal tissues without signs of liver toxicity [41].

Commenting on the possible reasons why these results differ from those published by Rich et al., the authors pointed out that interspecies differences between the Yucatan mini-pig and the domestic pig may affect animal sensitivity to the vector and/or the procedure.

In our study, we were able to deliver AAV9-GFP constructs in domestic pigs and obtain live offspring using a minimally invasive ultrasound-guided injection. We demonstrated the efficiency of this technique, resulting in a widespread biodistribution of the vector not only in peripheral tissue such as liver, heart, muscle, lung, kidney, and spleen, but also in different areas of CNS. Although technically challenging, this protocol is highly clinically relevant and could be easily translated to pregnant women.

Despite different gene therapy studies reported AAV9 toxicity in preclinical models and in clinical trials, particularly when administering high doses, we did not observe signs of hepatic, cardiac, or renal toxicity, or signs of neuroinflammation.

The necroscopic analysis of the two stillborn GFP+ piglets (#783 and #793) showed no signs of preterm death in utero (i.e. livor mortis, rigidity, signs of autolysis, putrefaction, maceration).

In our farm, the number of stillborn in unassisted births ranges from 2 to 4 for litters with 10 to 14 piglets. This average value is reflected in what we observed in these IUFGT experiments. Therefore, it is plausible that the two stillborn GFP piglets could be the result of random events naturally occurring during birth. However, a more extensive analysis on a higher number of pregnancy will be needed to identify and understand the exact causes of death, albeit these do not appear to be due to acute toxic/inflammatory events in our preliminary proof-of concept studies.

Considering the episomal nature of AAV9 – which causes dramatic dilution during cell division – coupled with the rapid increase in the body weight of piglets in the first month of life (from ~1.4 kg to 8 kg), the dosage that was injected in the #720 and #725 pigs, was probably insufficient in ensuring a longterm significant transgene expression.

Previous studies have reported that maternal pre-existing immunity, including anti-AAV neutralizing antibodies and T-cell responses, can cross the placenta or be transferred via milk postpartum, potentially affecting vector efficacy and neonatal immune responses [19, 42].

We examined the possibility of maternal immune activation and passive transfer of anti-AAV antibodies to the offspring, however post-intervention analysis revealed no seroconversion in treated sows, indicating that the procedure did not trigger a detectable maternal humoral immune response. This suggests a low

probability of maternal antibody transmission to the fetuses via the placenta or through colostrum. Furthermore, piglets born from these pregnancies did not exhibit detectable levels of anti-AAV antibodies, supporting the notion that systemic exposure of the dam to the vector was negligible.

All together, these results suggest that the low GFP copies detected in the tissues of one-month-old animals (#720, #725) are not due to the virus neutralization by the immune response, corroborating the hypothesis above that the low dosage used (1.2×10^{12} VG/ kg) and the rapid growth resulted in a notable dilution of the episomal viral genome in tissues. As for the brain, although neurons are post-mitotic, glial precursors and other supporting cell populations remain mitotically active at late gestation and may contribute to dilution of non-integrating episomal AAV genomes. Additionally, transcriptional silencing of the viral cassette due to epigenetic modifications, particularly in CNS tissues, has been observed in several animal models [42].

Another plausible explanation could be that in our model, vectors were delivered via intracardiac or umbilical vein injection. These routes may result in preferential vector delivery to high-perfusion organs (e.g., liver, heart), potentially limiting the number of viral particles reaching the brain. Unlike direct intraventricular or intracisternal injection, systemic routes rely on the ability of the vector to traverse the blood-brain barrier (BBB), which, although still permeable during late gestation, may exhibit increased selectivity at the time of injection as compared to earlier fetal stage.

CONCLUSION

While challenges such as off-target effects and long-term safety assessments warrant continued investigation, the evidence presented in this study underlies the efficacy and the safety of this therapeutic approach in the perinatal period. These results instill optimism for the prospect of implementing gene therapies in utero to prevent or correct many genetic diseases, specifically multisystem disorders such as mitochondrial diseases [43]. As we stand on the cusp of a new era in medicine, marked by the prospect of intervening in the earliest stages of human development, the findings presented herein contribute to the foundation upon which the future of IUFGT can be built. With careful consideration of ethical implications, rigorous safety protocols, and continued refinement of techniques, this innovative therapeutic approach may usher in a paradigm shift in the management of genetic disorders, offering renewed hope to families facing the challenges of congenital diseases.

DATA AVAILABILITY

Supporting Information is available from the author.

REFERENCES

1. Melchiorri D, Pani L, Gasparini P, Cossu G, Ancans J, Borg JJ, et al. Regulatory evaluation of Glybera in Europe — two committees, one mission. Nat Rev Drug Discov. 2013;12:719.
2. Russell S, Bennett J, Wellman JA, Chung DC, Yu ZF, Tillman A, et al. Efficacy and safety of voretigene neparvovec (AAV2-hRPE65v2) in patients with RPE65 -mediated inherited retinal dystrophy: a randomised, controlled, open-label, phase 3 trial. Lancet. 2017;390:849–60.
3. Mendell JR, Al-Zaidy S, Shell R, Arnold WD, Rodino-Klapac LR, Prior TW, et al. Single-dose gene-replacement therapy for spinal muscular atrophy. N Engl J Med. 2017;377:1713–22.
4. Ten Ham RMT, Walker SM, Soares MO, Frederix GWJ, Leebeek FWG, Fischer K, et al. Modeling benefits, costs, and affordability of a novel gene therapy in Hemophilia A. HemaSphere. 2022;6:e679.
5. Hemgenix - A gene therapy for hemophilia B. Med Lett Drugs Ther. 2023;65:9–10.
6. Delandistrogene moxeparvovec (Elevidys) for Duchenne muscular dystrophy. Med Lett Drugs Ther. 2023;65:159–60.
7. Schwab ME, Shao S, Zhang L, Lianoglou B, Belter L, Jarecki J, et al. Investigating attitudes toward prenatal diagnosis and fetal therapy for spinal muscular atrophy. Prenat Diagn. 2022;42:1409–19.
8. Deyle DR, Russell DW. Adeno-associated virus vector integration. Curr Opin Mol Therapeutics. 2010;11:442.
9. Wang D, Tai PWL, Gao G. Adeno-associated virus vector as a platform for gene therapy delivery. Nat Rev Drug Discov. 2019;18:358–78.
10. Collins LT, Ponnazhagan S, Curiel DT. Synthetic biology design as a paradigm shift toward manufacturing affordable adeno-associated virus gene therapies. ACS Synth Biol. 2023;12:17–26.
11. Ronzitti G, Gross DA, Mingozzi F. Human immune responses to adeno-associated virus (AAV) vectors. Front Immunol. 2020;11:670.
12. Di Donfrancesco A, Massaro G, Di Meo I, Tiranti V, Bottani E, Brunetti D. Gene therapy for mitochondrial diseases: current status and future perspective. Pharmaceutics. 2022;14:1287.
13. Waddington SN, Peranteau WH, Rahim AA, Boyle AK, Kurian MA, Gissen P, et al. Fetal gene therapy. J Inher Metab Disea. 2024;47:192–210.
14. MacKenzie TC. Future AAVenues for in utero gene therapy. Cell Stem Cell. 2018;23:320–1.
15. Bose SK, Menon P, Peranteau WH. In utero gene therapy: progress and challenges. Trends Mol Med. 2021;27:728–30.
16. David AL, McIntosh J, Peebles DM, Cook T, Waddington S, Weisz B, et al. Recombinant adeno-associated virus-mediated in utero gene transfer gives therapeutic transgene expression in the sheep. Hum Gene Ther. 2011;22:419–26.
17. Mattar CNZ, Nathwani AC, Waddington SN, Dighe N, Kaeppel C, Nowrouzi A, et al. Stable human FIX expression after 0.9G intrauterine gene transfer of self-complementary adeno-associated viral vector 5 and 8 in macaques. Mol Ther. 2011;19:1950–60.
18. Mattar CN, Waddington SN, Biswas A, Johana N, Ng XW, Fisk AS, et al. Systemic delivery of scAAV9 in fetal macaques facilitates neuronal transduction of the central and peripheral nervous systems. Gene Ther. 2013;20:69–83.
19. Mattar CNZ, Gil-Farina I, Rosales C, Johana N, Tan YYW, McIntosh J, et al. In utero transfer of adeno-associated viral vectors produces long-term factor IX levels in a cynomolgus macaque model. Mol Ther. 2017;25:1843–53.
20. Pekrun K, Stephens CJ, Gonzalez-Sandoval A, Goswami A, Zhang F, Tarantal AF, et al. Correlation of antigen expression with epigenetic modifications after rAAV delivery of a human factor IX variant in mice and rhesus macaques. Mol Ther. 2024;32:2064–79.
21. Lunney JK, Van Goor A, Walker KE, Hailstock T, Franklin J, Dai C. Importance of the pig as a human biomedical model. Sci Transl Med. 2021;13:eabd5758.
22. Quadalti C, Brunetti D, Lagutina I, Duchi R, Perota A, Lazzari G, et al. SURF1 knockout cloned pigs: early onset of a severe lethal phenotype. Biochim Biophys Acta Mol Basis Dis. 2018;1864:2131–42.
23. Langel SN, Paim FC, Alhamo MA, Buckley A, Van Geelen A, Lager KM, et al. Stage of gestation at porcine epidemic diarrhea virus infection of pregnant swine impacts maternal immunity and lactogenic immune protection of neonatal suckling piglets. Front Immunol. 2019;10:727.
24. Hordeaux J, Hinderer C, Goode T, Katz N, Buza EL, Bell P, et al. Toxicology study of intra-cisterna magna adeno-associated virus 9 expressing human alpha-L-iduronidase in rhesus macaques. Mol Ther Methods Clin Dev. 2018;10:79–88.
25. Hinderer C, Katz N, Buza EL, Dyer C, Goode T, Bell P, et al. Severe toxicity in nonhuman primates and piglets following high-dose intravenous administration of an adeno-associated virus vector expressing human SMN. Hum Gene Ther. 2018;29:285–98.
26. Muhuri M, Maeda Y, Ma H, Ram S, Fitzgerald KA, Tai PWL, et al. Overcoming innate immune barriers that impede AAV gene therapy vectors. J Clin Investig. 2021;131:e143780.
27. Perez BA, Shutterly A, Chan YK, Byrne BJ, Corti M. Management of neuroinflammatory responses to AAV-mediated gene therapies for neurodegenerative diseases. Brain Sci. 2020;10:119.
28. Chand DH, Sun R, Diab KA, Kenny D, Tukov FF. Review of cardiac safety in onasemnogene abeparvovec gene replacement therapy: translation from preclinical to clinical findings. Gene Ther. 2023;30:685–97.
29. Breous E, Somanathan S, Bell P, Wilson JM. Inflammation causes loss of adeno-associated virus-mediated transgene expression in mouse liver. Gastroenterology. 2011;141:348–357.e3.
30. He Y, Hwang S, Ahmed YA, Feng D, Li N, Ribeiro M, et al. Immunopathobiology and therapeutic targets related to cytokines in liver diseases. Cell Mol Immunol. 2021;18:18–37.
31. Silver E, Argiro A, Hong K, Adler E. Gene therapy vector-related myocarditis. Int J Cardiol. 2024;398:131617.
32. Wang JH, Gessler DJ, Zhan W, Gallagher TL, Gao G. Adeno-associated virus as a delivery vector for gene therapy of human diseases. Sig Transduct Target Ther. 2024;9:78.

33. Vaisitti T, Peritore D, Magistroni P, Ricci A, Lombardini L, Gringeri E, et al. The frequency of rare and monogenic diseases in pediatric organ transplant recipients in Italy. Orphanet J Rare Dis. 2021;16:374.
34. Murray CJL, Lopez AD. Measuring the global burden of disease. N Engl J Med. 2013;369:448–57.
35. Mai CT, Isenburg JL, Canfield MA, Meyer RE, Correa A, Alverson CJ, et al. National population-based estimates for major birth defects, 2010–2014. Birth Defects Res. 2019;111:1420–35.
36. WHO Birth defects. 2022. Available from: https://www.who.int/news-room/fact-sheets/detail/birth-defects.
37. Peddi NC, Marasandra Ramesh H, Gude SS, Gude SS, Vuppalapati S. Intrauterine fetal gene therapy: is that the future and is that future now? Cureus. 2022;14(2):e22521.
38. Mattar CNZ, Chan JKY, Choolani M. Gene modification therapies for hereditary diseases in the fetus. Prenatal Diagn. 2023;43:674–86.
39. Deweerdt S. Some genetic diseases cause damage even before a child is born. The answer to these devastating conditions could lie in gene therapy delivered while the baby is still in the womb. Sci Am. 2019;320:s4–6.
40. Rich KA, Wier CG, Russo J, Kong L, Heilman PL, Reynolds A, et al. Premature delivery in the domestic sow in response to in utero delivery of AAV9 to fetal piglets. Gene Ther. 2022;29:513–9.
41. Dave A, Berkowitz CL, Luks VL, White BM, Palanki R, Carpenter MD, et al. Comment on: premature delivery in the domestic sow in response to in utero delivery of AAV9 to fetal piglets. Gene Ther. 2023;30:232–5.
42. Rahim AA, Wong AMS, Hoefer K, Buckley SMK, Mattar CN, Cheng SH, et al. Intravenous administration of AAV2/9 to the fetal and neonatal mouse leads to differential targeting of CNS cell types and extensive transduction of the nervous system. FASEB J. 2011;25:3505–18.
43. Adelizzi A, Giri A, Di Donfrancesco A, Boito S, Prigione A, Bottani E, et al. Fetal and obstetrics manifestations of mitochondrial diseases. J Transl Med. 2024;22:853.

ACKNOWLEDGEMENTS

AA, ADD, IDM, VT, and DB are part of the Center for the Study of Mitochondrial Pediatric Diseases (http://www.mitopedia.org) funded by the Mariani Foundation. VT is a member of the European Reference Network for Rare Neuromuscular Diseases (ERN EURO-NMD). We thank Dr. Lorena Zentilin and all the staff of the AAV Vector Unit, International Centre for Genetic Engineering and Biotechnology (ICGEB) in Trieste for their support in the AAV production.

AUTHOR CONTRIBUTIONS

DB, ADD, AA, EB: manuscript writing and figure generation. DB, NP, SB, AG, AP, MB, RD and CG: in vivo procedures and animal testing. ADD, AA, EB, CS and EC: methodology. GM, IDM, VT and EB: manuscript revision. DB, NP: conception, manuscript writing, final approval of manuscript.

FUNDING

This research was funded by Fondazione Regionale per la Ricerca Biomedica (Regione Lombardia-FRRB) (Project ID 1740526 to DB) and by Fondazione Telethon (Project ID n. GMR23T2152 to DB). EB was supported by the European Joint Programme on Rare Diseases (EJP RD) H2020, grant n_ EJPRD20-010. We acknowledge financial support under the National Recovery and Resilience Plan (NRRP), Mission 4, Component 2, Investment 1.1, Call for tender No. 104 published on 2.2.2022 by the Italian Ministry of University and Research (MUR), funded by the European Union – NextGeneration EU–Project CUP B53D23018710001, Grant Assignment Decree No. n. 1110 adopted on 20/07/2023 by the Italian Ministry of University and Research (MUR) (to EB); Fondazione Telethon (Project ID GSA23F002 to EB), Italian Foundation A.M.Me.C. (to EB).

COMPETING INTERESTS

The authors declare no competing interests.

ETHICS APPROVAL AND CONSENT TO PARTICIPATE

All procedures involving the use of animals in this study were approved by the Local Ethics Committee of Avantea, carried out under the Italian Law (D. Lgs 26/2014) and EU directive 2010/63/EU regulating animal experimentation, and approved by relevant national authorities (Ministry of Health project n° 367/2022-PR). All the animal studies were done according to the ARRIVE guidelines.

CONSENT FOR PUBLICATION

All authors agree to publish this study.

ADDITIONAL INFORMATION

Supplementary information The online version contains supplementary material available at https://doi.org/10.1038/s41434-025-00551-8.

Correspondence and requests for materials should be addressed to Nicola Persico or Dario Brunetti.